

Pteridines  
Vol. 20, Special issue, pp. 163-167

## Crystal Structures of Substrate- and Sulfate-Bound Mouse Thymidylate Synthase

Anna Dowierciał<sup>1</sup>, Adam Jarmuła<sup>1</sup>, Wojciech Rypniewski<sup>2</sup>, Monika Sokołowska<sup>3</sup>, Tomasz Frączyk<sup>1</sup>, Joanna Cieśla<sup>1</sup>, Wojciech Rode<sup>1§</sup>

<sup>1</sup>Nencki Institute of Experimental Biology, Polish Academy of Sciences, Warszawa, Poland

<sup>2</sup>Institute of Bioorganic Chemistry, Polish Academy of Sciences, Poznan, Poland

<sup>3</sup>International Institute of Molecular and Cell Biology, Polish Academy of Sciences, Warszawa, Poland

### Abstract

Crystal structures of mouse thymidylate synthase (mTS), liganded with either 2'-deoxyuridine 5'-monophosphate (dUMP) or the sulfate anion, have been determined and deposited in Protein Data Bank under the accession codes 3IHH and 3IHI, respectively. The structures show a strong overall similarity to the corresponding structures of rat (rTS) and human (hTS) thymidylate synthases. The loop 175-191, corresponding to the hTS loop 181-197, populates the active conformation, with catalytic Cys 189 buried in the active site and directed toward C(6) of the pyrimidine ring of dUMP. Another loop, 41-47, differs in conformation from the corresponding loop 47-53 in unliganded human enzyme. It folds due to electrostatic attraction between Arg 44 and the sulfate/dUMP phosphate and partly covers the entrance to the active site.

**Key words** : Thymidylate synthase (EC 2.1.1.45)  
thymidylate synthase, 3IHH, 3IHI

### Introduction

Thymidylate synthase (TS) is ubiquitous among species and is one of the most conserved enzymes known so far. It catalyzes the reductive methylation of 2'-deoxyuridine 5'-monophosphate (dUMP) in the presence of the folate cofactor N<sup>5</sup>, N<sup>10</sup>-methylene tetrahydrofolate (mTHF) serving as an one carbon donor and reductant, to form deoxythymidine monophosphate (dTMP) and dihydrofolate. Since the reaction is the only *de novo* source of dTMP required for DNA synthesis, TS is an important target in chemotherapy, as its inhibition leads to apoptosis of dividing cells. Numerous derivatives of either dUMP or mTHF have been examined as TS inhibitors and potential anticancer drugs, and

several have been in clinical use for years.

TS is a dimer, composed of ~30-37 kDa monomers. The first step of the reaction catalyzed by TS is the nucleophilic addition of the active site cysteine (residue 189 in mTS) to the nucleotide pyrimidine C(6). The position and orientation of dUMP binding are essential at this stage of catalysis, the former secured by anchoring the nucleotide 5'-phosphate via several conservative hydrogen contacts from both TS subunits, and the latter promoted by the hydrogen bonding between the conserved asparagine (Asn220 in mTS) and both O<sup>4</sup> and N(3)-H moieties of the pyrimidine ring. Properly bound dUMP provides the binding surface for the cofactor, resulting in the formation of the ternary complex TS – dUMP – mTHF.

Among many TS crystal structures deposited in the Protein Data Bank (PDB), only those representing human and rat TS [1-8] are of

<sup>§</sup>Correspondence : Dr. Wojciech Rode, T: +48-22-589-2477; F: +48-22-822-5342; Email: w.ode@nencki.gov.pl

metazoan origin. Unlike in other known TS structures, human TS loop 181–197 was observed to populate two conformers, one of them, apparently inactive, stabilized by a pair of hydrogen bonds from Arg163 to the carbonyls of Ala191 and Leu192. As mTS, containing Lys157 corresponding to Arg163 in hTS, has been hypothesized unable to populate the inactive conformer [2], learning the crystal structure of the mouse enzyme was of interest.

## Materials and Methods

### Reagents

K/Na tartrate, PEG 3350, PEG 4000, Li<sub>2</sub>SO<sub>4</sub>, dUMP were purchased from Sigma, dithiothreitol (DTT) was from Carl Roth GmbH.

### Overexpression of mouse thymidylate synthase

The mTS coding region was cloned into pPIGDM4+stop vector, expressed as HisTag-free protein in thymidylate synthase-deficient TX61<sup>-</sup> (a kind gift from Dr. W. S. Dallas) *E. coli* strain and purified as previously described (9). Phosphatase inhibitors (50 mM NaF, 5 mM Na-pyrophosphate, 0.2 mM EGTA, 0.2 mM EDTA and 2 mM Na<sub>3</sub>VO<sub>4</sub>) were present in the purification buffers. TS activity was measured either spectrophotometrically [10] or with the use of the tritium release assay [9]. The final preparation was highly homogeneous, as judged by SDS/PAGE analysis of samples containing up to 40 µg protein. Its specific activity (the tritium release assay) was 1.75 µmol min<sup>-1</sup> mg protein<sup>-1</sup> at 37°C.

### Crystallization and data collection

Purified protein was dialyzed against 5 mM Tris HCl buffer, pH 7.5, containing 5 mM DTT, and then concentrated using Amicon Centricon centrifugal filter. Crystals were grown by the vapor diffusion method in the hanging drops at 4°C at the following conditions. For mTS alone, equal volumes of the protein (15 mg/ml) and well solutions were mixed and allowed to equilibrate with 0.5 ml of the well solution, containing 0.1 M Tris HCl, pH 8.5, 0.2 M Li<sub>2</sub>SO<sub>4</sub> and 25% (w/v) PEG 4000. For mTS-dUMP complex, a drop of the protein solution (25 mg/ml, containing 5.9 mM dUMP) was mixed with an equal volume of the well solution and allowed to equilibrate with 0.5 ml of well solution, containing 0.2 M K Na Tartrate and 20% PEG 3350. The crystals were transferred for a few seconds to cryoprotectant

solution containing either mother liquor and 25% butanediol (mTS-dUMP) or 30% glycerol (mTS alone), and flash-cooled in N<sub>2</sub> vapors.

X-ray diffraction data were collected from three single flash-frozen crystals at the Max-Lab Lund University Synchrotron using X-rays with wavelengths of 1,038 and 0,908 Å.

### Data processing, Structure determination and refinement

Data were processed with Denzo and Scalepack [12]. Both structures were determined by molecular replacement carried out with the CCP4 package [13], using the rat TS ternary complex without ligands as the search model. The crystal structures of mTS and mTS-dUMP were determined at resolutions of 1,94Å and 1,7Å, respectively. The correctness of the two structures was evaluated using Sfccheck & Procheck from the CCP4 suite. Some X-ray data and model refinement parameters are summarized in Table 1.

Table 1 : Summary of the X-ray data and model refinement

	mTS	mTS-dUMP
Resolution [Å]	1.94	1.7
Number of reflections	66 011	201 240
All atoms	4 932	14 789
Space group	C2	C2
R-value (%)	22.0	24.8
R <sub>free</sub> -value (%)	26.9	29.5
rms bond	0.022	0.019
rms angle	1.9	1.8
Beamline	1911-2	1911-5

## Results and Discussion

The structures, consisting of one and three dimers per asymmetric part of the unit cell for mTS and mTS-dUMP, respectively (Figure 1 and Figure 2), showed an overall similarity to the corresponding structures of hTS and rTS, as expected for proteins with highly conserved primary structures. The Cα RMSD values with respect to the crystal structures of hTS and rTS (both TS-dUMP-Tomodex complexes) are 0.49, 0.47, 0.35 and 0.50 Å for mTS vs. hTS, mTS-dUMP vs. hTS, mTS vs. rTS and mTS-dUMP vs. rTS, respectively.

The molecule of dUMP was bound in a manner similar to that observed in the corresponding

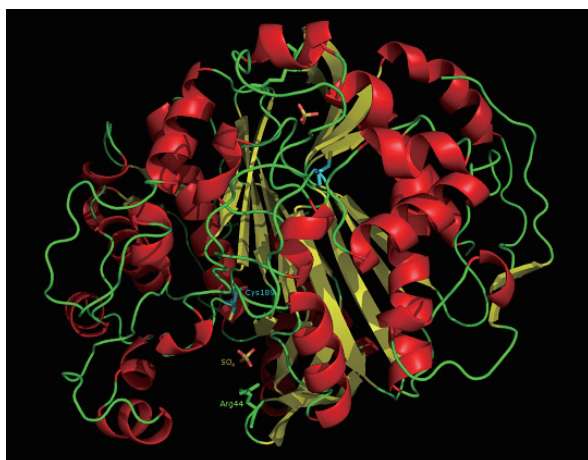


Figure 1 : Mouse thymidylate synthase (chain A) with sulfate anions ( $\text{SO}_4^{2-}$ ) bound inside the active sites (chains A and B). The protein is colored by secondary structure (helices in red, sheets in yellow, loops in green).

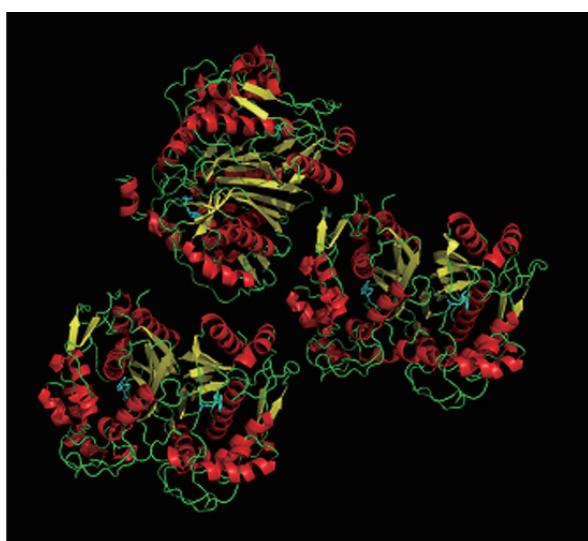


Figure 2 : Crystal structure of mouse TS complexed with the substrate, dUMP. Six subunits are shown, with ligands (blue) present in the active sites.

complexes of other mammalian and bacterial TSs, with the ligand anchored in the active site by several H-bonds to its phosphate moiety from four arginines from both subunits of the enzyme dimer (Arg44 and Arg209 from one subunit and Arg169' and Arg170' from the other subunit) and a single serine (Ser210). The orientation of dUMP was secured by H-bonds between the conserved Asn220 and the O<sub>4</sub> and N(3)-H moieties of the pyrimidine ring. The active site in the mTS structure held a single sulfate anion, bound at nearly the same location as dUMP phosphate moiety in the mTS-dUMP structure and stabilized by H-bonds with the pair of arginine

residues (Arg170' and Arg209) from the quartet coordinating the phosphate in the other structure.

The hTS loop 181-197 can populate two major conformations, active and inactive, related to each other by a 180 ° rotation. While in the former conformation, catalytic cysteine 195 locates itself in the active site, directed toward C(6) of the pyrimidine ring of dUMP (with which it forms the thiol adduct), in the latter Cys195 is more than 10 Å away from the foregoing location, directed toward the dimer interface of the enzyme. The equilibrium between both conformations has been shown to depend on the presence of either phosphate/sulfate ions, driving the equilibrium toward the inactive conformation, or dUMP, driving it toward the active conformation.

In the mTS-dUMP structure, loop 175-191, equivalent to human loop 181-197, populates the active conformation, with catalytic Cys189 located at a close, but non-covalent distance from dUMP. Interestingly, in the mTS structure, loop 175-191 populates the same (active) conformation, although the active site does not contain dUMP. Of note is that it does contain sulfate anion.

In hTS, the inactive conformer is stabilized by a pair of hydrogen bonds from Arg163 to the carbonyls of Ala191 and Leu192. The presence of lysine, instead of arginine, at the position 157 in mTS (equivalent to hTS 163) disallows



Figure 3 : Superimposition of the loops 175-191, from mTS-dUMP (lime), containing catalytic Cys189 inside the active site (active conformation), and 181-197, from hTS (blue), with catalytic Cys195 outside the active site (inactive conformation). The rest of the structure of mTS-dUMP (except loop 175-191) is shown in green.

the occurrence of the corresponding hydrogen bonding (with Ala185 and Leu186) due to a shorter side chain and lower adaptability to multiple H-bonding of the former, compared to the latter residue, as concluded from the comparison of the mTS and hTS crystal structures (Figure 3). This observation supports the hypothesis of Lovelace *et al* [2].

The structures of both mTS and mTS-dUMP, liganded with sulfate and dUMP, respectively, differ from unliganded hTS in the conformation of the loop 41-47 (hTS 47-53) (Figure 4). In the liganded systems, loop 41-47 partly covers the entrance to the active site, placing the side chain of Arg44 sticking out toward the sulfate/dUMP phosphate. In the absence of ligands, no strong electrostatic attraction exists between double negatively charged sulfate/phosphate and positively charged Arg50, resulting in loop 47-53 uncovering the entrance and extending away from the active site.

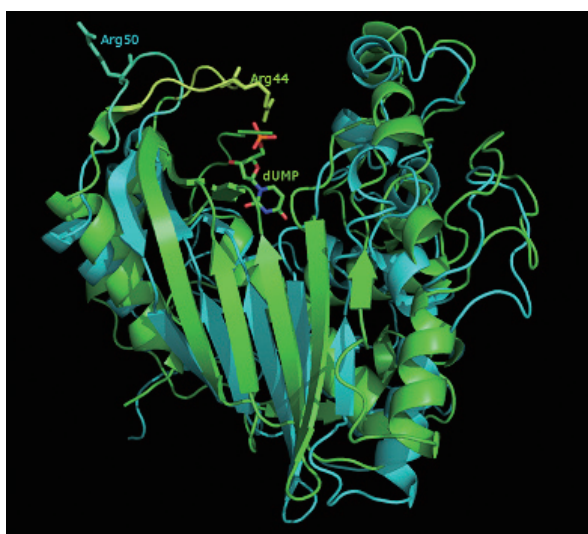


Figure 4. Superimposition of mTS-dUMP subunit A (green) and human R163K TS form 1 subunit A (blue). Different conformations of the corresponding loops 41-47 (mTS) and 47-53 (hTS) in the ligand-bound mTS and ligand-free hTS.

## Acknowledgments

Supported by the Ministry of Science and Higher Education (grant no. N301 3948 33).

## References

- Gibson L M, Lovelace L L, Lebioda L. The R163K Mutant of Human Thymidylate Synthase Is Stabilized in an Active Conformation: Structural Asymmetry and Reactivity of Cysteine 195. *Biochemistry* 2008; 47: 4636-4643.
- Lovelace L L, Gibson L M, Lebioda L. Cooperative Inhibition of Human Thymidylate Synthase by Mixtures of Active Site Binding and Allosteric Inhibitors. *Biochemistry* 2007; 46: 2823-2830.
- Lovelace L L, Minor W, Lebioda L. Structure of human thymidylate synthase under low-salt conditions. *Acta Cryst* 2005; D61: 622-627.
- Almog R, Waddling C A, Maley F, Maley G, Van Roey P. Crystal structure of a deletion mutant of human thymidylate synthase  $\Delta(7-29)$  and its ternary complex with Tomudex and dUMP. *Protein Science* 2001; 10: 988-996.
- Phan J, Steadman D J, Koli S, Ding W C, Minor W, Dunlap R B, Berger S H, Lebioda L. Structure of Human Thymidylate Synthase Suggests Advantages of Chemotherapy with Noncompetitive Inhibitors. *J. Biol. Chem* 2001; 276: 14170-14177.
- Phan J, Koli S, Minor W, Dunlap R B, Berger S H, Lebioda L. Human Thymidylate Synthase Is In the Closed Conformation When Complexed with dUMP and Raltitrexed, an Antifolate Drug. *Biochemistry* 2001; 40: 1897-1902.
- Schiffer C A, Clifton I J, Davisson V J, Santi D V, Stroud R M. Crystal structure of human thymidylate synthase: a structural mechanism for guiding substrates into the active site. *Biochemistry* 1995; 34: 16279-16287.
- Sotelo-Mundo R R, Ciesla J, Dzik J M, Rode W, Maley F, Maley G F, Hardy L W, Montfort W R. Crystal Structures of Rat Thymidylate Synthase Inhibited by Tomudex, a Potent Anticancer Drug. *Biochemistry* 1999; 38: 1087-1094.
- Ciesla J, Golos B, Walajtys-Rode E, Jagielska E, Plucienniczak A, Rode W. The effect of Arg209 to Lys mutation in mouse thymidylate synthase. *Acta Biochim. Pol* 2002; 49: 651-658.
- Wahba A, Friedkin M. The Enzymatic Synthesis of Thymidylate. *J. Biol. Chem* 1962; 237: 3794-3801.
- Rode W, Kulikowski T, Kedzierska B, Jastreboff M, Shugar D. Inhibition of mammalian tumour thymidylate synthetase by 5-alkylated 2'-deoxyuridine 5'-

- phosphates. *Biochem. Pharmacol* 1984; 33: 2699-2705.
12. Otwinowski Z, Minor W. Processing of X-ray Diffraction Data Collected in Oscillation Mode. *Methods in Enzymology*, Volume 276: *Macromolecular Crystallography* 1997; part A: 307-326.
13. Collaborative Computational Project, Number 4. The CCP4 Suite: Programs for Protein Crystallography. *Acta Cryst* 1994; D50: 760-763.

